communications

Fabrication via Electrochemical Oxidation of Self-Assembled Monolayers and Site-Selective Derivatization of Surface Templates**

*Stephanie Hoeppener and Ulrich S. Schubert**

The technological impact of magnetic materials in various fields of technology has fueled sustained research into the magnetic properties of different materials. As a result, novel phenomena, such as for example, the giant magnetoresistance (GMR) effect[1,2] and tunneling magnetoresistance[2] have been discovered and are currently integrated into devices, such as magnetic random access memory (MRAM) devices,[3] and will contribute to the further success of magnetic devices. With improving structuring techniques that allow the fabrication of magnetic structures with decreasing device dimensions additional properties of such structures become accessible and offer new possibilities for the effective construction of new devices.[4] Even with common magnetic materials, tremendous developments have been achieved to enlarge and speed-up magnetic data-storage capacities in the last decades and significant economical benefits are based on their rapid development.[5] Therefore research efforts address crucially the task of pushing the size limits of individual storage bits to a minimum. This is regarded as a key issue for fundamental and applied research.

The investigation of magnetic properties can be performed by a variety of powerful techniques;[6] in particular, magnetic force microscopy (MFM)[7] has contributed to a better understanding of the properties of magnetic materials.[8] This technique allows the high-resolution imaging of the magnetic properties and is therefore suitable even for the investigation of size and shape effects on the magnetic properties of small, nanodimensional objects.[9] Small magnetic nanoparticles might provide many new possibilities. Besides the synthesis of these particles, a convenient way to arrange them in a suitable, most preferably ordered, structure on a surface is also desired. Spontaneous self-organization might fulfill this key requirement only in certain systems and therefore it is necessary to combine structuring techniques and the assembly of defined nanoparticles.

Besides the state-of-the-art top-down structuring approaches, which can be efficiently utilized to generate structures down to a certain size limitation, newly developed bottom-up lithography approaches have attracted much interest because of the small ultimate device dimensions that can potentially be achieved. Microcontact printing (μCP)[10] and more recently also dip-pen nanolithography (DPN)[11] have provided suitable tools for this design approach and the first examples of creating magnetic patterns with nanometer dimension have been demonstrated.[12] Magnetic structures have also been fabricated with an approach that uses electroless metal deposition on scanning force microscopy (SFM) patterned substrates.[13] We report here on the site-selective fabrication of Fe particles on nanopatterned self-assembled monolayer templates, which are generated by probe-based electrooxidative nanolithography.

By applying a sufficient voltage to the monolayer, a chemical change in the surface functions is induced due to the oxidation of the surface-terminated methyl groups of the monolayer,[14,15] leaving the remaining part of the monolayer completely unaffected. This maintains the useful surface properties of the monolayer, such as hydrophobicity, chemical stability, and mechanical robustness. The surface templates exemplify a chemical addressability that can be used in terms of bottom-up nanofabrication. Different modification schemes for the guided assembly of additional material on such surface patterns, as well as the chemical derivatization of the surface templates by means of chemical modification routines have been developed. Such modifications of the surface templates can involve, for example, the use of additional self-assembled layers, to provide alternative chemical functionality,[15] or they are directly used to selectively bind or adsorb functional nanoparticles, such as Au nanoparticles.[16] The chemically inert self-assembled monolayer, which can easily be activated by electrochemical oxidation, allows the sequential orthogonal functionalization and thus the stepwise, hierarchical assembly of complex structures. Another modification routine uses the site-selective in situ generation of nanoparticles directly on the surface pattern.[15,17] The latter approach is used here to generate functional magnetic nanoparticles on predefined surface patterns, which are subsequently analyzed by means of MFM. Thus it is possible to use SFM as a fabrication tool as well as for the analysis of nanodimensional magnetic structures.

The fabrication of nanodimensional magnetic structures (Scheme 1) utilizes the local electrochemical oxidation of a well-defined, densely packed self-assembled monolayer consisting of *n*-octadecyltrichlorosilane (OTS) molecules. These multivalent chlorosilane molecules are hydrolyzed in the presence of water and spontaneously bind covalently to, for example, silicon substrates bearing a native oxide layer.[18] Besides the covalent linkage to the substrate, additional bond formation is provided by the silanol functions of adjacent molecules, thus resulting in a partial, lateral cross-linking within the monolayer and therefore in the formation of mechanically rigid monolayer-coated substrates (Scheme 1A).

[*] Dr. S. Hoeppener, Prof. U. S. Schubert
Eindhoven University of Technology
Laboratory of Macromolecular Chemistry and Nanoscience
P.O. Box 513, 5600 MB Eindhoven (The Netherlands)
Fax: (+31) 40-2474186
E-mail: u.s.schubert@tue.nl
Prof. U. S. Schubert
Center for Nanoscience (CeNS)
Universität München
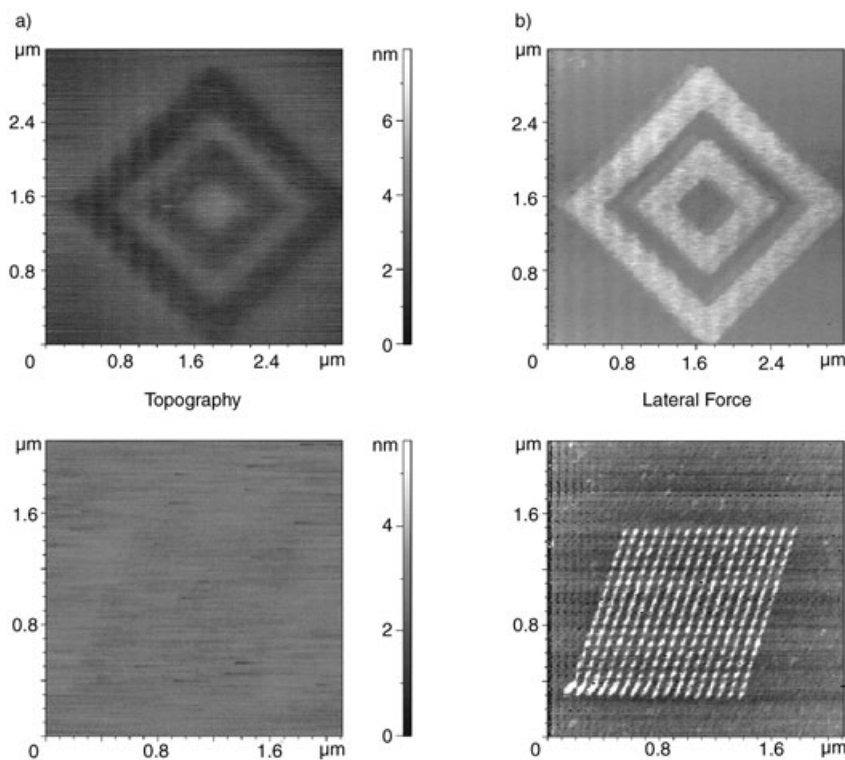Geschwister-Scholl-Platz 1
80333 München (Germany)
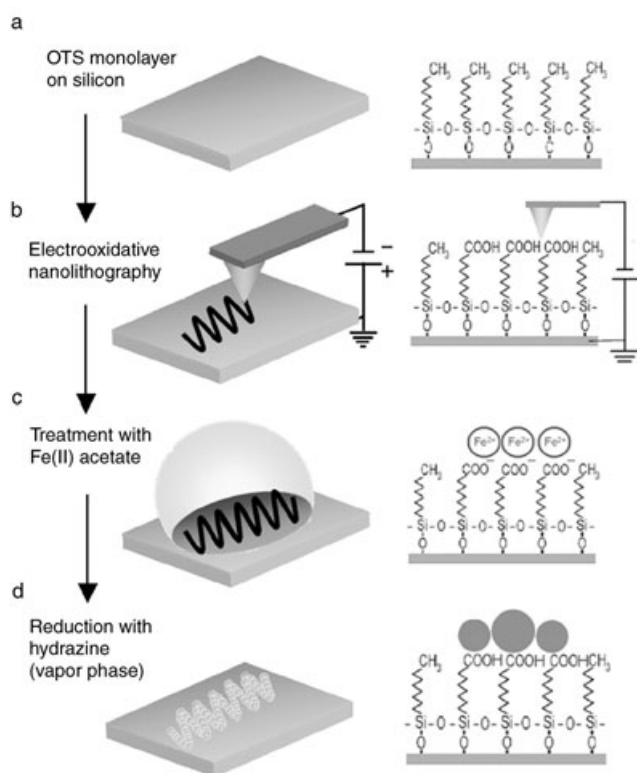
Scheme 1. Schematic representation of the fabrication approach of magnetic nanostructures on OTS self-assembled monolayers (a) by means of electrooxidative nanolithography (b) followed by the site-selective in situ derivatization of the surface structures (c, d).

in these regions, thus exhibiting significantly stronger friction forces in contrast to the surrounding, still hydrophobic, unmodified OTS monolayer. Due to the almost unaffected topography signal, it can be concluded that the monolayer itself is not destroyed by the electrooxidation process. The origin of the small negative contrast in the corresponding topography signal has recently been assigned to the cross-coupling of the friction and topography signal and is therefore regarded as an artifact of the measurement mode.[19] The chemically heterogeneous surface with chemically active surface patterns and the chemically inert, remaining OTS layer provides a suitable template structure to guide the site-selective generation of magnetic nanoparticles. This process is initiated by the binding of, for example, Fe^{II} ions to the −COOH functions (Scheme 1C). Subsequent reduction[17] of the Fe salt attached to the surface template results in the generation of Fe nanoparticles (Scheme 1D) as depicted in Figure 2.

The coverage of the template is remarkably high and the particle film appears to be homogeneous, as demonstrated by the rhombic structure composed of an array of individual writing points, which are arranged sufficiently close to each other. The apparent particle height is very uniform, forming a film of typically 6–7 nm thickness (Figure 2c), whereas the number of particles per unit surface area depends crucially on the dimension of the template structures itself. This effect is exemplified in Figure 2d, which exhibits two different kinds of dots, sequentially inscribed on the OTS template within the same surface area. The smaller

It was demonstrated that applying a negative tip bias voltage will result in the local conversion of the surface exposed −CH₃ groups of the octadecyl chain into −COOH functions. Provided that the voltage is applied by a conductive SFM tip, structure sizes with a typical linewidth of ≈20 to 50 nm can be generated, depending critically on the tip dimensions and patterning conditions, such as the applied voltage, writing speed, humidity, and so on.[19] Figure 1 depicts a typical result of such an electrooxidative patterning (compare also with Scheme 1B).

The conversion of −CH₃ functions into −COOH groups generates a strong difference in surface properties, which can be easily detected by means of contact mode imaging, whereby the lateral force signal is recorded. Bright features in the lateral force images indicate the surface areas where a negative tip bias voltage was applied. The monolayer is rendered hydrophilic

Figure 1. a) Topography and b) lateral force microscopy images of the OTS self-assembled monolayer after the electrooxidative template inscription. The bright lateral force contrast and the almost unaffected topography contrast are regarded as an indication of the successful conversion of surface-terminated −CH₃ groups into −COOH functions.
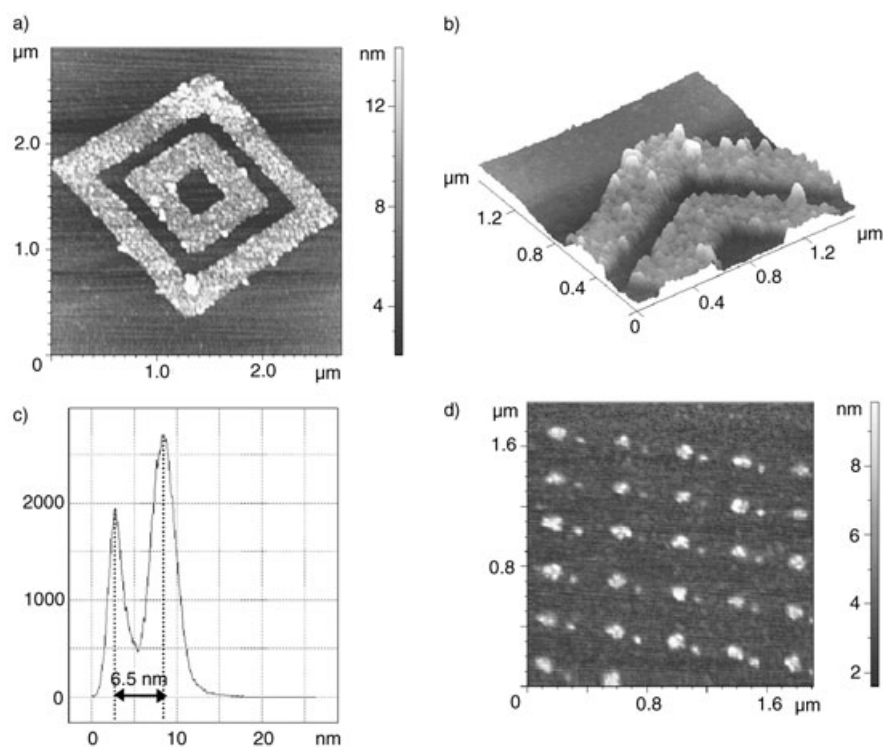
Figure 2. Topography SFM tapping-mode images of Fe nanoparticles generated in situ on chemically active −COOH-terminated surface templates. a, b) Densely covered surface templates generated in a raster-like oxidation process. c) Histogram of the observed particle heights. A 250 × 250 nm^2 area of the structure depicted in (a) was chosen for the statistical analysis. d) The size-dependant coverage of the surface template is correlated with the different capability of the surface templates to accumulate iron ions from the solution and is therefore dependent on their individual size.

process is applicable because of the hydrophobic surface properties of the unmodified OTS surface, which are maintained in the surroundings of the template structures.

MFM is used to verify the magnetic properties of these nanoparticles. This two-pass scanning technique, which uses a magnetic SFM tip, allows the sensing of the magnetic-field distribution of the magnetic nanostructures with high resolution. In the course of these investigations two different experimental conditions were investigated: the examination of the magnetic properties of the nanoparticle array in the presence of an external magnetic field, and in the absence of such external fields, respectively.

The magnetization of the investigated Fe particles, which constitute a relatively soft magnetic material, are expected to be easily manipulated or reoriented by means of an external magnetic field. The field can be applied either by mounting the sample on a strong magnet, certainly at the expense of

dots were created using a faster oxidation process that led to significantly smaller oxidized areas of, in this case, ≈20 nm; the larger points exhibit an average diameter of ≈45 nm. In the latter case, 3–5 Fe nanoparticles can be found, whereas the majority of the smaller dots host only a single Fe particle, due to the significantly reduced area that can potentially be loaded with Fe^{II} ions. Only a few of these smaller dots exhibit a higher loading with more than one nanoparticle.
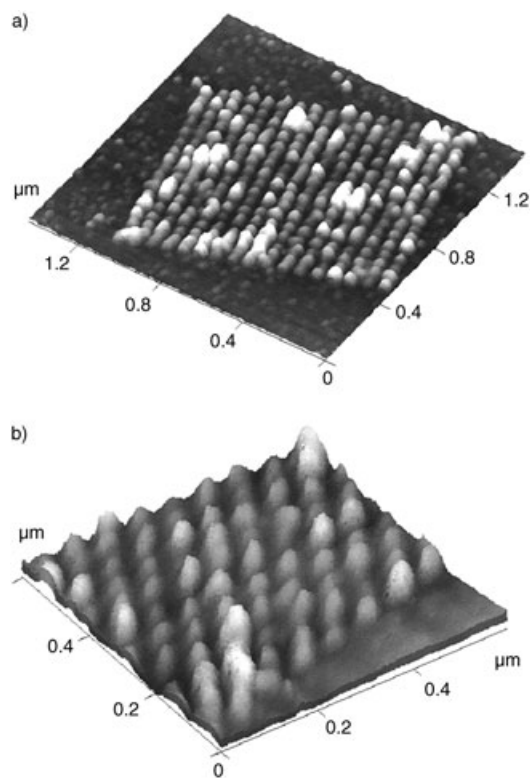
Such arrangements of individually placed nanoparticles allow the convenient generation of magnetic nanostructures of arbitrary shape and dimension range, especially designed for the requirements of the particular application, for example, for storage device structures. Figure 3 depicts a 17 × 17 dot array (1.0 μm^2 patterned area), which hosts individual Fe nanoparticles. The next-neighbor spacing between two particles is in this case only 50 nm.

The apparent particle size is in the 25 nm range, as could be demonstrated with an ultrasharp whisker SFM tip that shows the very uniform formation of nanoparticles on the template structure. The individual particles are clearly separated from each other and the particle height appears to be uniform. The stability of these particles is remarkably high, as they are stable even against adhesion tape, which can conveniently be used to clean the substrate from contaminations that might appear on the unmodified surface after the wet-chemical modification routine. This cleaning

Figure 3. Uniformly covered array of individual iron particles with a next-neighbor spacing of ≈50 nm. Imaging is performed in tapping mode with a Multimode SFM.

not being able to manipulate the strength of the field, or by using a small coil underneath the sample that creates a variable magnetic field, which can be controlled by an external voltage/current source. MFM investigations performed in the presence of such an external magnetic field are depicted in Figure 4 a, b.
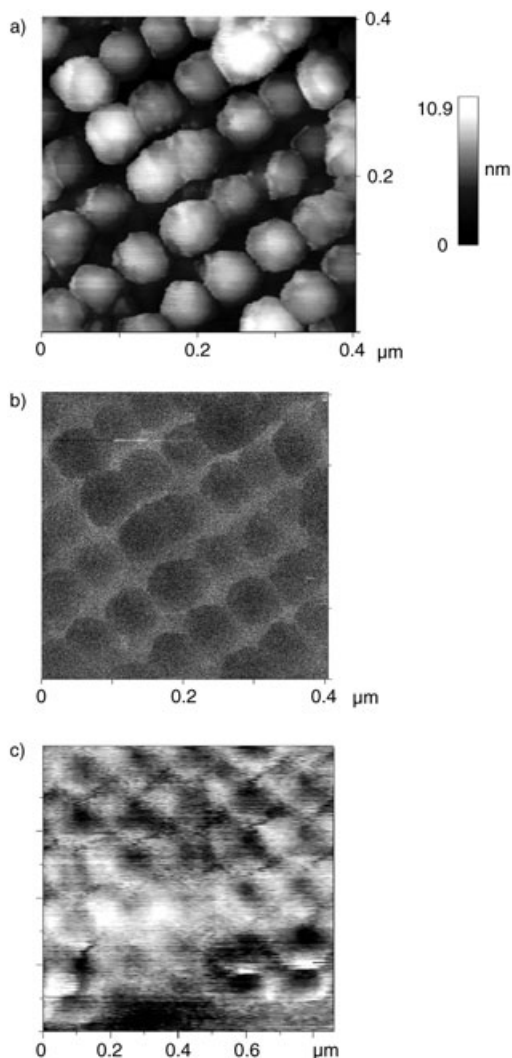
Figure 4. Topography and magnetic force images of the 17 × 17 dot array depicted in Figure 3. a) The limited resolution due to the enlarged tip size (Co/Cr-coated SFM tip) is evident in the apparently larger particle size observed in the topography image. b) The magnetic orientation of the nanoparticles was investigated in the presence of an external magnetic field, which reorientates the magnetic field of the individual particles in a uniform direction, as exemplified by the similar contrast observed in the magnetic force measurements. c) In the absence of an external magnetic field, different magnetic orientations of the magnetic field of the individual particles are observed.

To guarantee that the magnetic image depicts pure information about the magnetic properties of the sample, a sufficiently large tip-to-sample distance of at least 100–250 nm was used to probe the magnetic interaction between a Co-

coated SFM tip and the sample. As a result of the large distance, it can be discounted that the tip touches the surface during the probing of the magnetic interaction and therefore the typical shift for the noncontact MFM image is reduced to 2° or even less (in contrast to >25° for normal tapping conditions).

Not only the relatively large distance between tip and sample in the magnetic imaging contributes to a reduced resolution of this imaging technique, but also the additional 20 nm chromium coating of the tips, which is used to prevent oxidation of the magnetic layer. Naturally such tips are not very sharp and the overall resulting tip curvature is expected to be in the ≈ 90 nm region. The reduced resolution of such SFM tips can be directly observed in Figure 4 a, which essentially depicts the topography of the same surface area that is also shown in Figure 3, there imaged with an ultrasharp SFM tip. Figure 4 b depicts the corresponding magnetic image recorded from this region in the presence of an external magnetic field, achieved in this case by mounting the sample on a relatively strong magnet. It can be observed that the contrast generated during the scan above the surface is the same for each magnetic particle. This uniform contrast is not observed when the measurements are performed without the presence of an external magnetic field as depicted in Figure 4 c. Different particles exhibit here a nonuniform magnetic-field distribution, as detected by the magnetic SFM tip. This is especially evident in the bottom row of particles, where particles with different magnetic orientation are observed next to each other. In the densely packed areas towards the center of this structure a folding of magnetic influences of different particles that are affecting the tip cannot be completely excluded due to the limited resolution of the tip (as discussed above).

The presented investigations prove the magnetic origin of the nanoparticles, which are generated in a highly reproducible derivatization process directly on the surface. Further investigations will concentrate on the detailed analysis of shape/size influences on the magnetic properties (such as domain boundaries) of different magnetic structures. The high particle density generated in this approach makes this derivatization technique also interesting for the fabrication of conducting nanostructures, which would open new possibilities in terms of functional device design that certainly will require the assembly of device features consisting of different materials. The construction of such multicomponent devices will benefit certainly from the easy and versatile lithography approach, and the possibility of the sequential functionalization of predefined surface areas to hierarchically assemble more complex device features.

One obvious drawback of the SFM-tip mediated electrooxidation approach is certainly the relatively slow inscription speed. Attempts to use the automatization of the SFM setup to copy thousands of individual structures without the necessity of intervention from the operator[20] or the use of multiple-tip arrays[21] might be able to tackle this problem. Another alternative, which has already been demonstrated, is to replace the SFM tip with electrically conductive stamps,[22] thus providing a convenient way to perform electrooxidative patterning in a parallel fabrication fashion.

communications

Experimental Section

n-Octadecyltrichlorosilane monolayers were prepared from dry bicyclohexyl (BCH) solution on freshly cleaned silicon wafers (Silicon Quest International; p-type, B-doped, $<100>$, 10–20 Ωcm) as described elsewhere.[17] The surface templates were inscribed in contact mode with Pt-coated SFM tips (μMasch) at a humidity of 45 % by applying -5 V voltage pulses to the tip for 0.1 ms or 0.01 ms on a Solver LS SFM (NT-MDT). Imaging was performed with a Solver P47H SFM (NT-MDT) or a Nanoscope IIIa Multimode system (Digital Instruments).

Particles were generated by immersing the substrate in an aqueous Fe^{II} acetate solution (2 mM) for 10 min, followed by copious rinsing with deionized water and drying in a stream of N_2. The particle formation was initiated by the subsequent reduction of the Fe ions in the vapor phase of hydrazine for 10 min. Final application of adhesion tape removes contamination and residues from the preparation process, leaving the Fe particles unaffected. Particle coverage could be improved by a repeated immersion of the substrate in Fe^{II} acetate solution and subsequent reduction steps.

[1] a) M. N. Baibich, J. M. Broto, A. Fert, F. Nguyen Van Dau, F. Petroff, P. Eitenne, G. Creuzet, A. Friederich, J. Chazelas, *Phys. Rev. Lett.* **1988**, *61*, 2472; b) Z. F. Lin, S. T. Chui, L. B. Hu, *Phys. Lett. A* **2004**, *332*, 115.

[2] A. Barthelemy, A. Fert, J. P. Contour, M. Bowen, V. Cros, J. M. De Teresa, A. Hamzic, J. C. Faini, J. M. George, J. Grollier, F. Montaigne, F. Pailloux, F. Petroff, C. Vouille, *J. Magn. Magn. Mater.* **2002**, *242–245*, 68.

[3] a) J. A. Katine, R. E. Fontana, *Introduction to Nanoscale Science and Technology* **2004**, 355; b) N. Pekas, M. D. Porter, M. Tondra, A. Popple, A. Jander, *Appl. Phys. Lett.* **2004**, *85*, 4783; c) H. Bruckl, M. Brzeska, D. Brinkmann, J. Schotter, G. Reiss, W. Schepper, P. B. Kamp, A. Becker, *J. Magn. Magn. Mater.* **2004**, *282*, 219.

[4] a) R. L. White, *J. Magn. Magn. Mater.* **2002**, *242–245*, 21; b) C. Tsang, T. Lin, S. MacDonald, M. Pinarbasi, N. Robertson, H. Santini, M. Doerner, T. Reith, V. Lang, T. Diola, P. Arnett, *IEEE Trans. Magn.* **1997**, *33*, 2866.

[5] D. N. Lambeth, D. E. Laughlin, S. Charap, L. L. Lee, P. Harllee, L. Tang, *Appl. Sci. Res.* **1997**, *338*, 767.

[6] a) E. Y. Vedmedenko, A. Kubetzka, K. von Bergmann, O. Pietzsch, M. Bode, J. Kirschner, H. P. Oepen, R. Wiesendanger, *Phys. Rev. Lett.* **2004**, *92*, 077207; b) G. Meyer, T. Crecelius, G. Kaindl, A. Bauer, *J. Magn. Magn. Mater.* **2002**, *240*, 76.

[7] a) Y. Martin, H. K. Wickramasinghe, *Appl. Phys. Lett.* **1987**, *50*, 1455; b) M. Bode, M. Dreyer, M. Getzlaff, M. Kleiber, A. Wadas, R. Wiesendanger, *J. Phys. C* **1999**, *11*, 9387.

[8] a) J. Martinek, J. Barnas, A. Fert, S. Maekawa, G. Schon, *J. Appl. Phys.* **2003**, *93*, 8265; b) A. Killinger, R. Hollinger, U. Krey, *J. Magn. Magn. Mater.* **2004**, *272–276*, 724.

[9] a) X. Zhu, P. Grütter, *MRS Bull.* **2004**, *29*, 457; b) R. D. Gomey, E. R. Burke, I. D. Mayergoyz, *J. Appl. Phys.* **1996**, *79*, 6441.

[10] Y. Xia, G. M. Whitesides, *Angew. Chem.* **1998**, *110*, 568; *Angew. Chem. Int. Ed.* **1998**, *37*, 550.

[11] D. S. Ginger, C. Zhang, C. A. Mirkin, *Angew. Chem.* **2004**, *116*, 30; *Angew. Chem. Int. Ed.* **2004**, *43*, 30.

[12] a) X. Liu, L. Fu, S. Hong, V. P. Dravid, C. A. Mirkin, *Adv. Mater.* **2002**, *14*, 231; b) L. Fu, X. Liu, Y. Zhang, V. P. Dravid, C. A. Mirkin, *Nano Lett.* **2003**, *3*, 757.

[13] a) D. I. Ma, L. Shirey, D. McCarthy, A. Thompson, S. B. Qadri, W. J. Dressick, M. S. Chen, J. M. Calvert, R. Kapur, S. L. Brandow, *Chem. Mater.* **2002**, *14*, 4586; b) S. L. Brandow, J. M. Calvert, E. S. Snow, P. M. Campbell, *J. Vac. Sci. Technol. A* **1997**, *15*, 1455; c) F. K. Perkins, E. A. Dobisz, S. L. Brandown, J. M. Calvert, J. E. Kosakowski, C. R. K. Marrian, *Appl. Phys. Lett.* **1996**, *68*, 550.

[14] R. Maoz, S. R. Cohen, J. Sagiv, *Adv. Mater.* **1999**, *11*, 55.

[15] R. Maoz, S. R. Cohen, J. Sagiv, *Adv. Mater.* **2000**, *12*, 725.

[16] a) S. Liu, R. Maoz, G. Schmid, J. Sagiv, *Nano Lett.* **2002**, *2*, 1055; b) D. Wouters, U. S. Schubert, *Langmuir* **2003**, *19*, 9033.

[17] S. Hoeppener, R. Maoz, S. R. Cohen, L. F. Chi, H. Fuchs, J. Sagiv, *Adv. Mater.* **2002**, *14*, 1036.

[18] J. Sagiv, *J. Am. Chem. Soc.* **1980**, *102*, 92.

[19] D. Wouters, R. Willems, S. Hoeppener, C. F. J. Flipse, U. S. Schubert, *Adv. Funct. Mater.* **2005**, in press.

[20] D. Wouters, U. S. Schubert, unpublished results.

[21] P. Vettiger, M. Despont, U. Drechsler, U. Durig, W. Haberle, M. I. Lutwyche, H. Rothuizen, R. Stutz, R. Widmer, G. K. Binnig, *IBM J. Res. Dev.* **2000**, *44*, 191.

[22] S. Hoeppener, R. Maoz, J. Sagiv, *Nano Lett.* **2003**, *3*, 761.